D11

TRANSONIC FLUTTER OF CONTROL SURFACES

By Albert L. Erickson

Ames Aeronautical Laboratory

The one-degree-of-freedom type of transonic flutter is a new flutter problem encountered in the transonic range in addition to the classical or two-or-more-degrees-of-freedom problem. It is intended in this paper to discuss only the one-degree-of-freedom case. This type of flutter results from some form of time delay. This time delay has been explained as being caused by separation resulting from the shock front across the wing. In the case of separation, flutter can be explained as being due to the periodic breakaway and reattachment of the flow about the airfoil, an effect similar to that which can be obtained at low speed on stalled airfoils due to high angle of attack or excessive thickness. It has also been considered, however, that due to the high velocities over the airfoil, changes in the hinge moment could be retarded during flutter so that an unstable condition might exist even without separated flow. Of course, in the actual case separation generally does occur; and it has been found that as separation becomes more severe the flutter becomes less violent in that the amplitude decreases. It should be noted that the one-degree-of-freedom type of flutter cannot be prevented by any of the standard flutter prevention methods which involve the uncoupling of mechanical movements. If the flutter is due to a time delay which does not necessarily involve separations, elimination of the aerodynamic force does not appear to be very feasible. Therefore, the solution of first importance involves the determining of the flutter frequency to be expected with any given system.

By use of the available experimental data, an empirical solution has been developed which appears to have sufficient merit to be of practical use. The problem involved has been set up in its simplest form and is shown in these first equations (fig. 1). The first equation is the simple one-degree-of-freedom equation with all the mechanical forces on the left side and the aerodynamic force shown as a single resultant on the right side. The solution of the equation used makes it necessary to determine the flutter frequency, a phase angle, and the magnitude of the hinge moment. With this equation the conditions for instability can be easily shown. In order to determine the flutter frequency some measure of the time lag is necessary. The basic parameter selected for indicating the time lag has been called the aerodynamic frequency and is based on the distance from the wing trailing edge to the minimum pressure point and on an assumed average velocity distribution after the shock which goes from slightly below a Mach number of 1 to free-stream velocity at the trailing edge. The equation then takes this form (fig. 1) with the constant K experimentally determined. The parameter was selected on the basis that impulses or changes

at the trailing edge could not get through the shock front outside of the boundary layer; this assumption is substantiated by steady-state results which show that deflections of a control have little effect on the flow in front of a shock wave. Therefore, the parameter appears to be a reasonable one in determining time lags. The type of analysis used assumes that the actual phase angle would be a direct function of the difference between the aerodynamic period and the flutter period which is the basis of this approximate phase-angle equation. The constant in the aerodynamic frequency parameter was determined for the most part from the results of one test and then checked against all other available data. In the basic test the phase angle for several conditions of flutter was determined by use of a shadowgraph system of visualizing shock and aileron motion. Figure 2 shows the type of shock pictures obtained. It was possible by analyzing a large number of these pictures to obtain the phase relationships as shown in figure 3. It was then assumed that, inasmuch as the time delays of pressure propagations would be greatest in moving from the trailing edge to the shock and much less when moving from the shock to the trailing edge, the phase relationship of the shock motion as shown must be an indication of the phase relationship of the hinge moment on the aileron. It was this type of information, obtained from a series of tests (table I), that was used actually to check the phase-angle equation. By use of the computed phase angle and the known mechanical parameters it was found that the dynamic resultant hinge-moment slope was the same as the static hinge-moment slope. Therefore, the magnitude of the dynamic hinge moment can be estimated from static data until more exact solutions are obtained. These results also show that increasing the separation causes a decreased flutter amplitude as was previously mentioned.

The equations developed have been checked for general correctness as to predicting flutter frequencies on six different models as shown in table II. It is believed that the wide range of frequencies involved makes the check quite reliable. It is interesting to note that the wing with the NACA 0012-64 section had internal aerodynamic balance and this balance was very effective in helping to prevent flutter, it being necessary to go to a Mach number of 0.875 to get any indication of flutter at all; and even then the flutter was not of a dangerous nature since a very small amount of damping such as might be in an ordinary control system would have stopped the flutter. (See table II.) The Langley Laboratory obtained the flutter of the control-surface type on the sweptback wing during rocket-propelled tests. Figure 4 shows the type wing and airfoil sections involved. The aerodynamic frequency was computed by use of the airfoil normal to the leading edge. The flutter range to be expected, as shown in table II, was found to be from 73 to 109 cycles per second. The actual test results shown in figure 5 show that the flutter range was from about 90 to 115 cycles per second. It is not believed that this one test is sufficient evidence to warrant the general use of the equations for sweptback-wing analysis, although it

is important to note that the sweepback merely delays the onset of flutter to Mach numbers above 1 in this case.

In order to explore and to understand further the one-degree-of-freedom transonic flutter, instantaneous pressure cells were installed on a test wing and the pressures were measured at several flutter frequencies. Figure 6 shows the type of pressure record obtained. The notations on the records indicate the position of the cell in percent chord and whether it is top or bottom surface. An oil damper was inserted in the system to control the amplitude, the damping force being measured by a strain gage. One cell shows a square-wave effect. It was found upon investigation that the shock wave passes over this cell and results in the very sharp changes. From these records, pressure-distribution changes at various points through the cycle were plotted as shown in figure 7. By following these records through a cycle it is possible to see the propagation of the pressure waves with time. The dotted lines indicate the lower surface and the solid lines, the upper. By use of the part of these plots over the aileron it was possible to integrate and to determine the instantaneous hinge moments due to the upper surface and the lower surface independently along with the resultant hinge moment as is shown in figure 8. This figure shows the instantaneous aileron angle plotted against the instantaneous hinge moment, the time lag causing the hysteresis effect. The area of this figure is a measure of the energy expended in overcoming the mechanical forces. The greater the time lag, the more open the figure becomes. It may be seen that subsonic flow is probably induced on the lower surface as the aileron goes down, that the lag effect disappears, and that no work is done. The upper surface shows a similar effect in that the energy loop becomes less open when the aileron is in the upper position. Other curves of this same nature have actually shown that at the lower Mach numbers or at lower angles of attack a certain amount of damping due to the lower surface occurs in this region. By using the maximum amplitudes measured and by setting the areas of these loops equal to the area of the ellipse that would do the same amount of work, the phase angles noted are determined. It is interesting to note that when the upper and lower surfaces are combined into the total hinge moment the result is a fairly uniform figure approaching closely the pure elliptic form. In the final plot the aileron motion and total hinge moment are plotted as a function of time to show the relative purity of the wave shapes. Generally speaking, it has been found that the relationships suggested by the empirical solution are in reasonable agreement with the results of the pressure tests. It has been indicated, however, that the actual lower-flutter frequency may be slightly less than that predicted by the present solution, although the exact lower limit is difficult to determine.

In conclusion it can be said that an empirical method has been developed that can be used to predict the flutter-frequency range, and

by knowing the mechanical characteristics of the control and the static hinge-moments the possibility of flutter occurring can be computed. Furthermore, there is as yet no indication that airfoil section can in itself have any effect in preventing flutter except that it should control the possible flutter-frequency range. It is also evident that inasmuch as static hinge moments are a measure of the dynamic hinge moments, internal aerodynamic balance can be sufficient to prevent a serious one-degree-of-freedom flutter problem.

BIBLIOGRAPHY

Brown, Harvey H., Rathert, George A., Jr., and Clousing, Lawrence A. : Flight-Test Measurements of Aileron Control Surface Behaviour at Supercritical Mach Numbers. NACA RM No. A7A15, 1947.

Spreiter, John R., Galster, George M., and Cooper, George E. : Flight Observations of Aileron Flutter at High Mach Numbers as Affected by Several Modifications. NACA RM No. A7B03, 1947.

Barmby, J. G., and Clevenson, S. A. : Initial Test in the Transonic Range of Four Flutter Airfoils Attached to a Freely Falling Body. NACA RM No. L7B27, 1947.

Erickson, Albert L., and Stephenson, Jack D. : Transonic Flutter of Control Surfaces. NACA RM No. A7F30, 1947.

[redacted]

TABLE I.

SUMMARY OF SHADOWGRAPH RESULTS

CONFIGURATION	AILERON MOTION, TOTAL (DEG.)	PHASE DIFF, ϕ (DEG.)	FREQUENCY f (cps)	MAX HINGE MOMENT H_o (FT.-LBS.)
STANDARD	18.4	67	21.2	1500
SPOILERS AT 0.50c	6.6	17	19.5	360
BUMPS AT 0.50c	18.6	51	21.2	1362
BUMPS AT 0.70c	9	54	19.4	570
TAPERED BUMP	16.0	25	20.8	1030

NACA

Ericson

TABLE II

SUMMARY OF FLUTTER RESULTS

AIRFOIL SECTION	RELATIVE RESTRAINT CONDITION	CHORD INCHES	COMPUTED FLUTTER FREQUENCY	ACTUAL FLUTTER FREQUENCY
65, - 213 a = 0.5	FIXED	56	24 TO 32	28, 32
65, - 213 a = 0.5	FREE	56	15 TO 24	15 TO 25
4412	FIXED	6	240	250
SYMETRICAL DOUBLE WEDGE	RESONANT	8	102	100
0012 - 64 EXTENDED TRAILING EDGE, 10.7% THICK	FREE	55	12 TO 18	15.6 TO 17.3
0012 - 64 EXTENDED TRAILING EDGE, 10.7% THICK	FIXED	55	18 TO 24	23
66 - 2X - 216 a + 0.6	FREE	65	18 TO 27	20
65 - 010 45° SWEPT WING	FREE	10	72 TO 109	90 TO 120

[redacted]

NACA

Erickson

[redacted]

$$I\ddot{\delta}_a + C\delta_a + K_m\delta_a = H_o \sin \omega t$$

$$\delta_a = \delta_{a_o} \sin (\omega t - \phi)$$

$$\tan \phi = \frac{C\omega}{K_m - I\omega^2}$$

$$f_a = \frac{a(1-M)}{2Kd}$$

$$\phi = \left(1 - \frac{f}{f_a}\right) 360°$$

NACA

Figure 1.- Equations used in the empirical solution of transonic control surface flutter

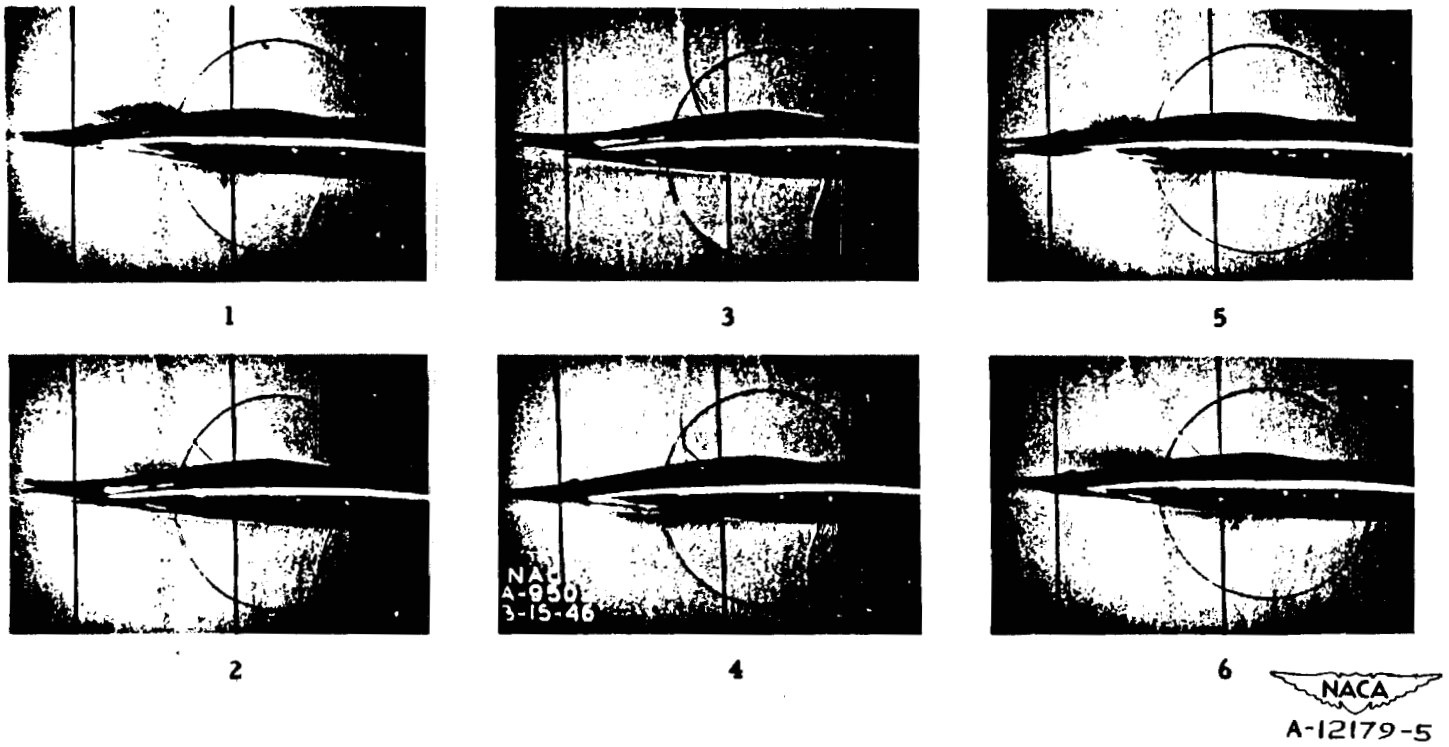

Figure 2.- Shadowgraphs of wing with aileron free.

Erickson

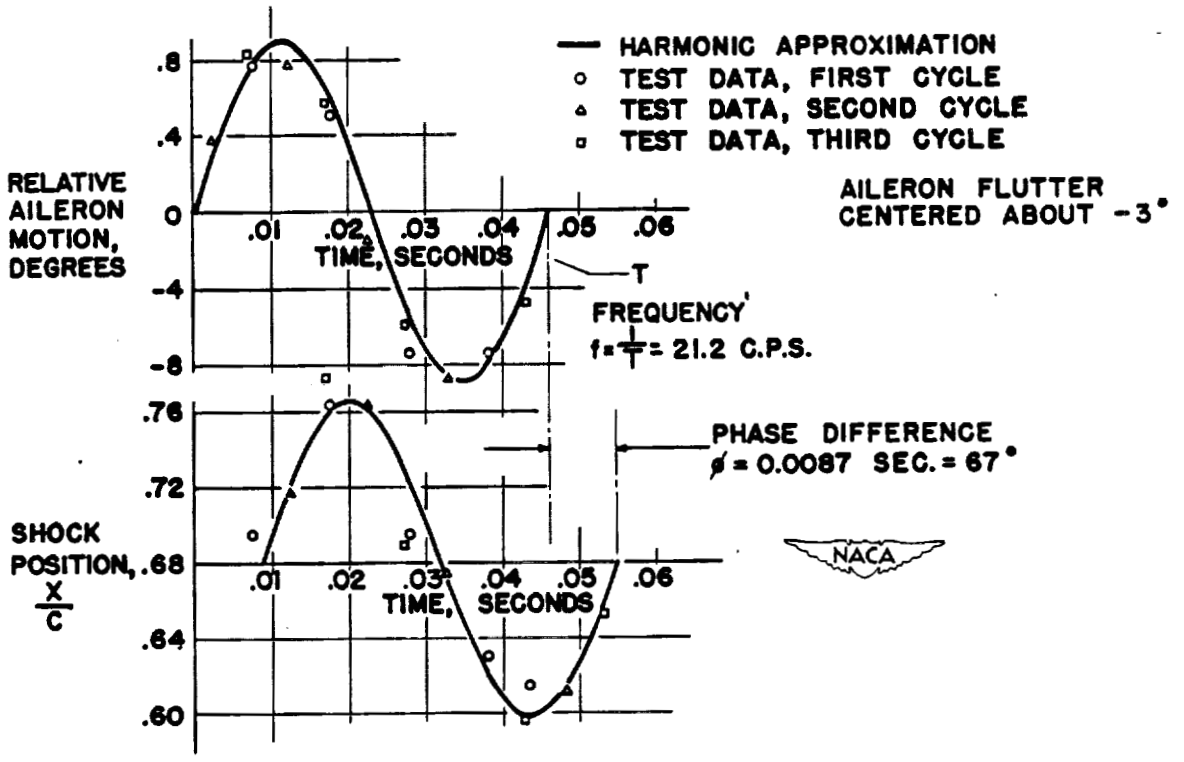

Figure 3.- Relative shock and aileron motion as a function of time.

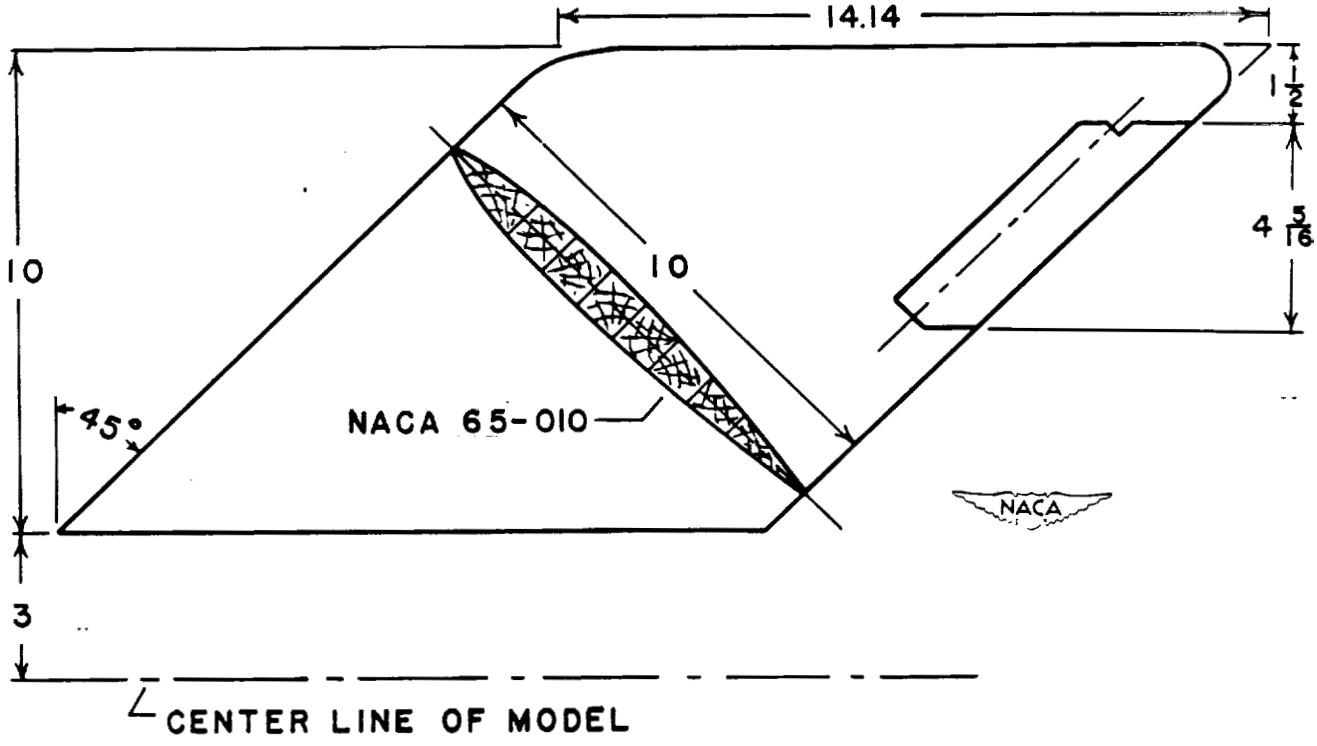

Figure 4.- Plan form of sweptback flutter model.

[redacted]

12(d)

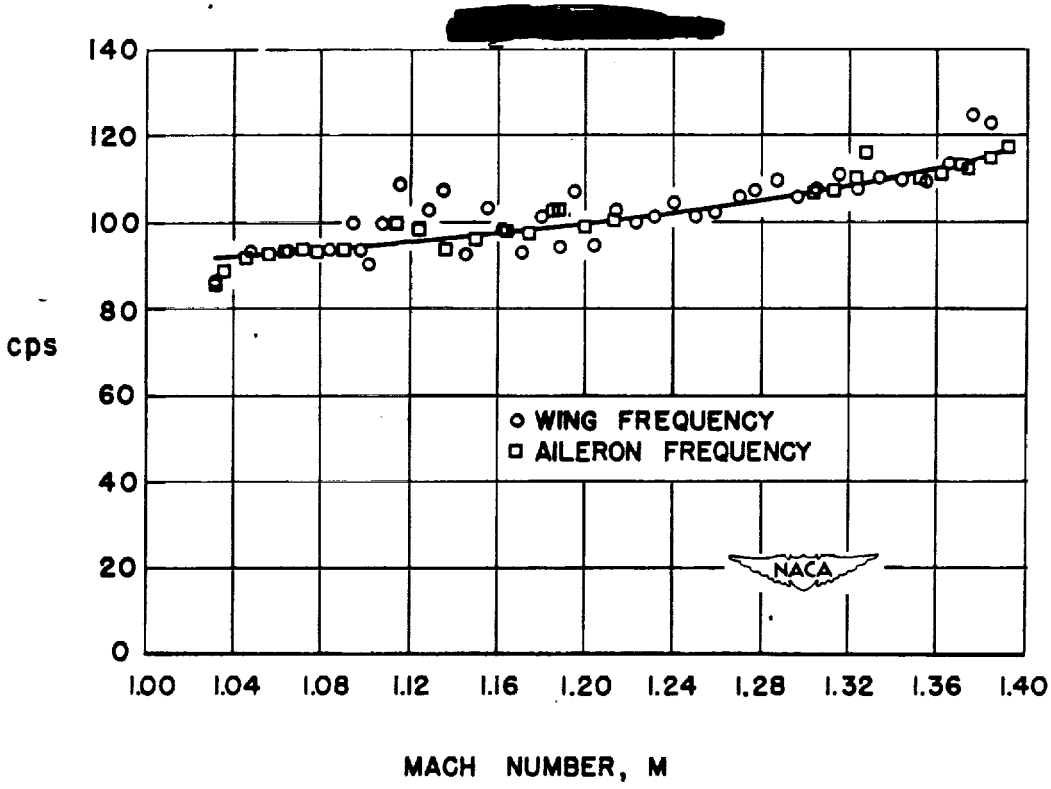

Figure 5.- Flutter results obtained with a sweptback wing.

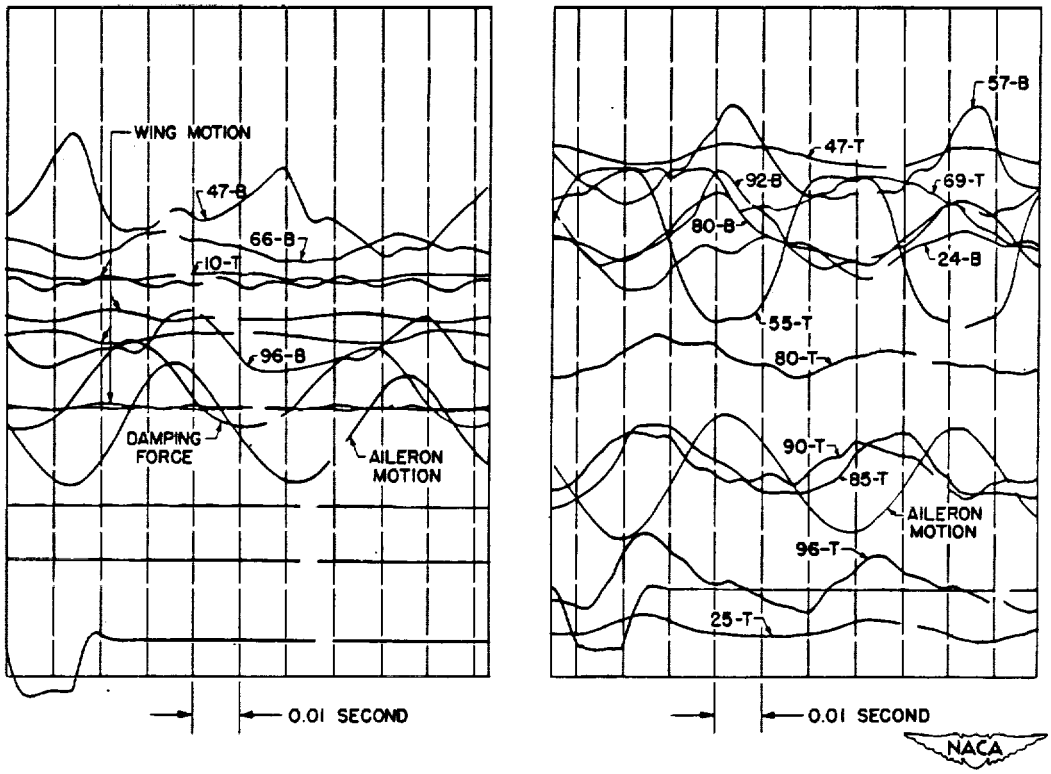

Figure 6.- Typical records obtained with instantaneous pressure recorders.

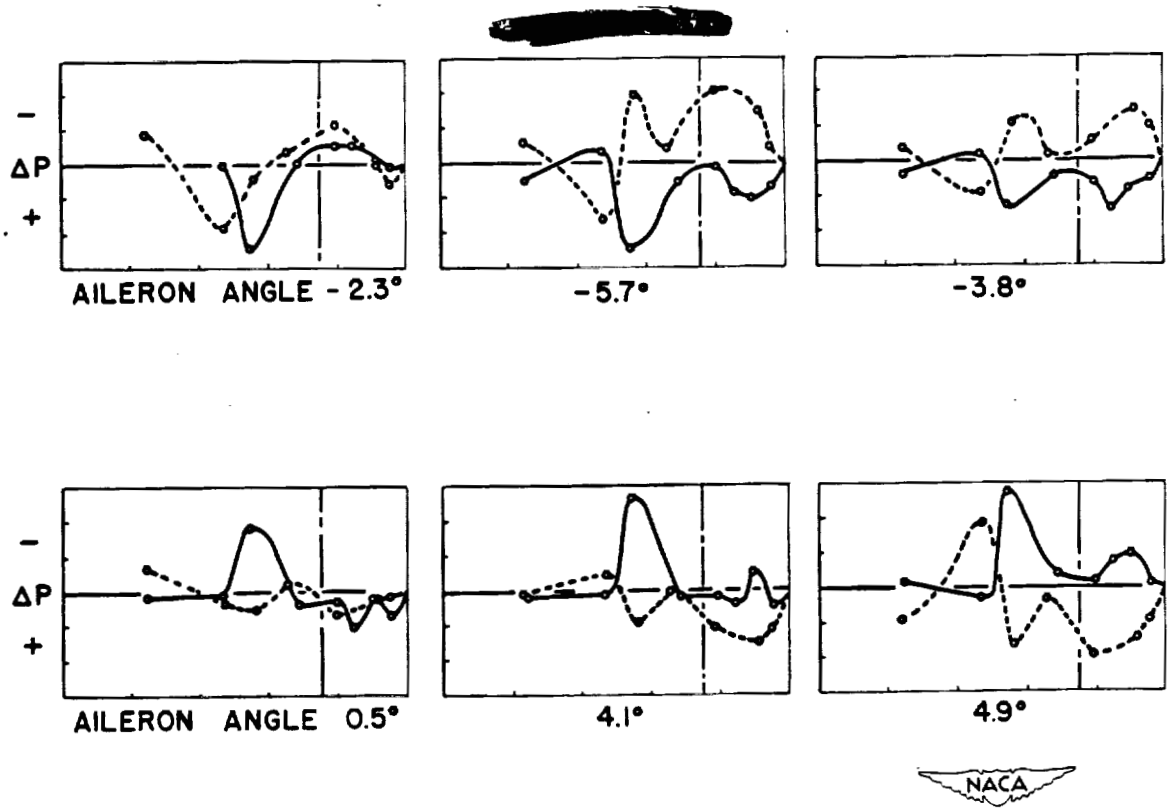

Figure 7.- Pressure-distribution changes at various points through a cycle.

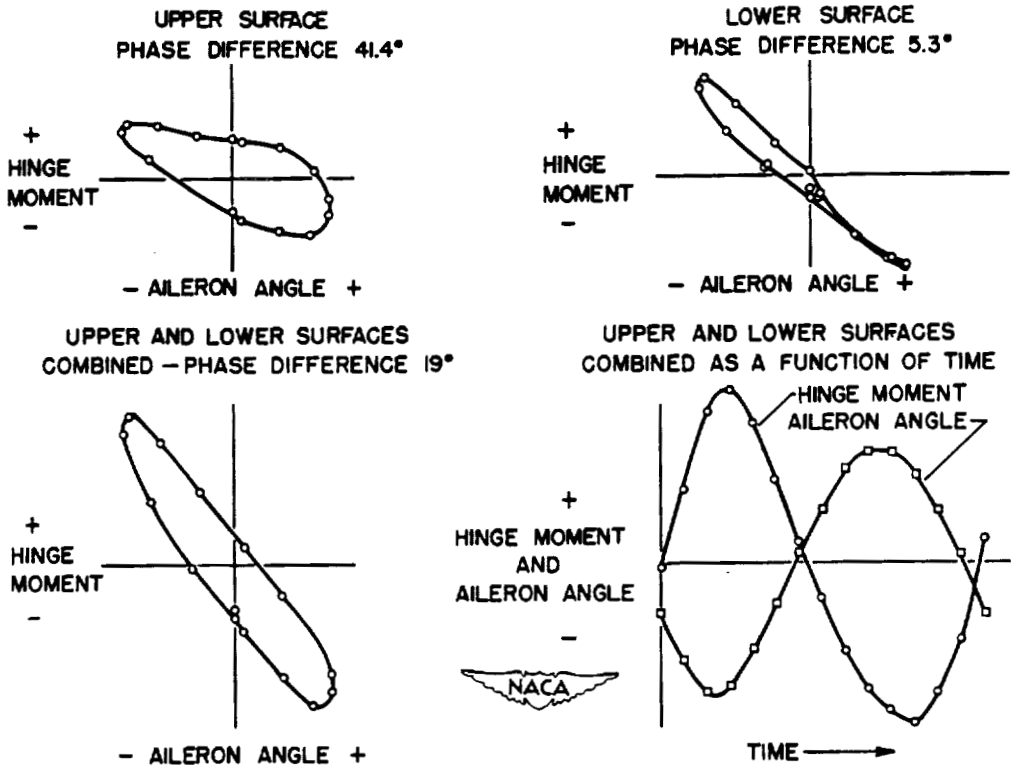

Figure 8.- Hinge-moment results obtained by the use of instantaneous pressure cells.

Erickson